

Combined VGG-LSTM with Gamma Correction for Pneumonia Type Classification based on Chest X-Rays

Nia Amelia, Riskyana Dewi Intan Puspitasari, Hasanuddin Al-Habib, and Elly Matul Imah

Abstract—Pneumonia is the second disease with the most patients being treated in the emergency department. Pneumonia can be distinguished based on its severity into viral and bacterial pneumonia. The coronavirus (COVID-19) has become a pandemic that spread globally. Panic during the pandemic has caused many people to self-diagnose and acknowledge common pneumonia as COVID-19. Despite having almost similar symptoms, not all pneumonia is COVID-19. Pneumonia is an inflammation of the lungs caused by bacteria, viruses, or fungi. In contrast, pneumonia in COVID-19 is caused by the SARS-CoV-2 virus. Early diagnosis of COVID-19 and pneumonia is crucial to perform the optimal treatment. A chest x-ray is a common way to detect pneumonia and is recommended for COVID-19. This study proposes a Pneumonia classification including a COVID-19 system based on X-Rays images using a combination of Visual Geometry Group (VGG) and Long Short Term Memory (LSTM) on chest X-ray images. We also applied gamma correction image enhancement to the thorax X-ray image. In the proposed system, VGG is used for feature extraction, and LSTM is used as a classifier. The experimental results show that the proposed system got an accuracy of 96.88% compared to previous state-of-the-art methods for pneumonia classification.

Index Terms—Pneumonia, covid-19, VGG, LSTM, classification.

I. INTRODUCTION

Pneumonia is an acute infection or inflammation in the lung tissue caused by various microorganisms such as bacteria, contagions, spongers, fungi, chemical exposure, or physical damage to the lungs. A study shows that pneumonia is the second disease with the most patients being treated in the emergency department [1]. Pneumonia can infect humans from various age groups and cause quite a high morbidity and mortality in both developed and developing countries, but most common in developing countries [2]. Indonesia's Health Profile data in 2020 also shows a high prevalence of pneumonia in children under five, that is, 3.55 per 100 children under five. This report means 3 to 4 out of 100 children under five suffer from pneumonia [3].

Pneumonia is divided into three categories; such community-acquired pneumonia (CAP) or pneumonia community, hospital-acquired pneumonia (HAP) and ventilator-associated pneumonia (VAP) that distinguished by the source of infection from pneumonia. In addition, pneumonia can be distinguished based on its severity into

viral pneumonia and bacterial pneumonia. Viral pneumonia is considered to be milder and has symptoms that occur gradually. While bacterial pneumonia is considered more severe, and symptoms can occur suddenly, especially in children. This type of pneumonia affects the lobes of the lungs that a person needs to be hospitalized [2].

During the COVID-19 outbreak in 2020, panic during the pandemic caused many people to self-diagnose and acknowledge common pneumonia as COVID-19. Despite having almost similar symptoms, not all pneumonia are COVID-19. Pneumonia is an inflammation of the lungs caused by bacteria, viruses, or fungi, and in contrast, pneumonia in COVID-19 is caused by the SARS-CoV-2 virus. Various studies have shown that the severity of COVID-19 pneumonia is higher than other types of pneumonia. Symptoms transitions in patients affected by COVID-19 Pneumonia will be faster and can cause fatal respiratory symptoms [4], [5], [6]. Pneumonia can commonly be identified by observing the chest X-ray (CTX) results [2]. On CTX, the doctor will see the infiltrate on a chest X-ray and diagnose pneumonia severity. A system that can diagnose pneumonia automatically is needed to make it easier for doctors to diagnose the infiltrates and the severity of the infected lungs. In addition to being fast, accurate, and precise, classification is needed to avoid misdiagnosis.

At present, the development of Artificial Intelligence has contributed to the medical world, especially in providing fast and accurate disease diagnoses [7]. Many researchers have proposed various based pneumonia and COVID-19 classification systems for Artificial Intelligent. Khuzani generated an optimal set of features from Chest-X Ray (CXR) images using dimensionality reduction methods and then used a machine learning classifier to distinguish COVID-19 Pneumonia and pneumonia cases with high accuracy and sensitivity [8]. Panwar used Deep Transfer Learning Algorithm to detect COVID-19 Pneumonia cases using chest X-Ray and CT Scan Images, also with Grad-CAM-based color visualization for better interpretation [9]. Oh used a patch-based convolutional neural network to generate segmentation on a small number of CXR Datasets for COVID-19 diagnosis [10]. Even combinations of algorithms have been applied to build a system with the best performance. Islam used a combination of deep learning algorithms such as Convolutional Neural Networks (CNN) for deep feature extraction and long short-term memory (LSTM) to detect COVID-19 automatically from featured extracted from CXR images [11], [12], [13]. In addition, Khan used hybrid learning from several modified pre-trained models to enrich feature

The authors are with the Data Science Department, State University of Surabaya, Indonesia e-mail: nia.18038@mhs.unesa.ac.id, elly-matul@unesa.ac.id.

Manuscript received January 21, 2023; accepted October 12, 2023.

space from Chest X-ray images [14].

Image enhancement plays an essential role in many fields, one of which is medical image processing to improve the quality of an image [15]. T. Rahman et al. have been comparing five image enhancement methods were compared, namely Histogram Equalization (HE), Contrast Limited Adaptive Histogram Equalization (CLAHE), Image Complement, Gamma Correction, and Balance Contrast Enhancement Technique (BCET). They used image enhancement to improve the performance of the Pneumonia classification system. The result is gamma correction, which is better than the other image enhancements technique, so we use this method in the study [16]. Gamma correction is an image enhancement technique that belongs to the Histogram Modified (HM) family of techniques obtained only by adaptively changing the gamma parameter [17].

Detecting COVID-19 using chest X-ray images is still challenging due to limited access to datasets and image quality, which can affect accuracy. The authors in [18], [19], [20] classify X-ray images into COVID and non-COVID cases. Meanwhile, COVID-19 also causes infection in the respiratory tract. In some cases, complications of COVID-19 can cause pneumonia [21]. Pneumonia caused by COVID-19 is often confused with non-COVID pneumonia because they share the same symptoms. However, based on study conducted by Pagliano et al. said that both have different clinical characteristics from other pneumonia [21].

Moreover, to find out these characteristics, further testing is needed to find out the difference, one of which is through identification on CT scan images [22]. Therefore, this study will also detect Viral Pneumonia and Bacterial Pneumonia in COVID and Non-COVID cases. Authors in [8] distinguished COVID-19 chest X-ray images from normal cases and pneumonia caused by other viruses. Hence, this study proposes a Pneumonia diagnosis system by classifying chest X-ray images into several various classes based on the previous study from 2 classes [12], [23], [24], 3 classes [25], [26], or 4 classes [27] including COVID-19. We provide the heatmap visualization of chest X-rays in every class to explore abnormality and severity in some areas. Several studies have also carried out transfer learning and compared it with various methods. From the research conducted by [28], [29], it is found that the transfer learning process using VGG produced the most significant performance compared to other pre-trained model. Therefore, we combined Gamma Correction to image enhancement on chest X-ray images with VGG feature extraction and Long Short-Term Memory (LSTM) network to diagnose the chest X-ray images with several classes, including COVID-19, Bacterial Pneumonia, Viral Pneumonia, and Normal. Our contribution is to create a new approach for Pneumonia classification which can improve the classification system on CXR images to produce a better performance evaluation than other state-of-the-art methods in Pneumonia and COVID-19 classification on CXR image.

II. METHODOLOGY

The stages of the Pneumonia classification system based on chest X-ray images in this study began with the data

TABLE I
RESEARCH DATA DISTRIBUTION

Class Label	Training	Test Data	Total
Bacterial Pneumonia	752	203	955
COVID-19	1029	237	1266
Normal	2854	714	3568
Viral Pneumonia	373	98	471
Total	5008	1252	6260

acquisition stage. The next step is data pre-processing, which aims to simplify the image model. The pre-processing carried out in this study includes resizing, filtering, and image enhancement. Furthermore, the images that have gone through the pre-processing stage will be partitioned into training and test data. After that, a model will be built using the training data to obtain a predictive model. The model performance in detecting Pneumonia is evaluated using testing data. The following evaluation metrics measure the performance of the proposed system in this study: confusion matrix, accuracy, sensitivity, specificity, and F1-Score.

A. Dataset

The input data used in this paper is Chest X-ray images obtained from the open dataset in COVID-19 Radiography Database from Kaggle [16]. This dataset was divided into four classes: Normal class, COVID-19 class, Bacterial Pneumonia class, and Viral Pneumonia. We split each class into data training and data testing with stratified random sampling with ratio 8:2, shown in Table 1.

B. Data Pre-Processing

In computer vision, the pre-processing stage is essential. Especially in medical digital images, the available medical images tend to be of poor quality. Therefore, a stage is needed for pre-processing to improve the quality of medical images [30], [31]. In this study, the proposed Pneumonia classification system uses data in the form of digital radiographic images. Therefore, the system must read the important information in the image. Several pre-processing techniques were applied in this study. These techniques include Resizing, Filtering, and Image Enhancement. Resizing is a technique of pre-processing that aims to change the pixel size. In this study, the thorax X-ray image was subjected to a resizing process, so the image size became 255×255 .

Technique Filtering aims to improve the image. In addition to resizing, the technique of pre-processing used is filtering. The reapplications filtering varies in images, including smoothing, sharpening, removing noise, and edge classification. However, in this study, the technique of filtering used is sharpening. Meanwhile, image enhancement is a technique of image processing that highlights essential information in an image and reduces or eliminates less critical information to improve image quality. In this study, the technique of Image Enhancement used is gamma correction.

C. Gamma Correction

Gamma Correction performs non-linear operations on image pixels. According to the internal map, Gamma Correction replaces pixel values to correct the image using the projection relationship between pixel values and gamma values. P represents the pixel values in the range $[0,255]$, Ω represents the angle values, Γ is the symbol of the set gamma value. x is a gray scale value pixel $x \in \rho$. Let x_m be the midpoint of the range $[0, 255]$. Linear map from group P to a group Ω defined as:

$$\phi : \rho \rightarrow \Omega, \Omega = \omega | \omega = \phi(x), \phi(x) = \pi x / (2x_m) \quad (1)$$

Pre-maps from Ω to ρ is defined as :

$$h : \Omega \rightarrow \Gamma, \Gamma = \{\gamma | \gamma = h(x)\} \begin{cases} h(x) = 1 + f_1(x) \\ f_1(x) = \text{acos}(\varphi(x)) \end{cases} \quad (2)$$

Suppose $\gamma(x) = h(x)$, the Gamma correction function is presented in equation (3), representing the result of the pixel correction value in gray scale. Whereas weighted factors based on these maps, the group can be associated with the pixel values of the group. The new pixel value is calculated with to the given Gamma value.

$$g(x) = 255 \times \left(\frac{x}{255} \right)^{\frac{1}{\gamma(x)}} \quad (3)$$

D. Classification

1) *Support Vector Machine(SVM)*: The SVM algorithm is one of the most widely used kernel-based learning algorithms in various machine learning applications, primarily image classification [32]. The primary purpose of this technique is to project a non-linear split sample to another higher dimensional space using various kernel functions. The performance of the SVM algorithm is highly dependent on the selection of kernel functions that can generate samples in the higher-dimensional feature space. Several kernel models can be used to build SVM algorithms, including Sigmoid, Radial Basis Function (RBF), Polynomial, and Linear in Eq (4)-(7), where $\kappa > 0$, $\vartheta < 0$. The kernel selection is generally selected by defining the existing model and then adjusting the kernel parameters K by techniques tuning.

Linear :

$$K(\vec{x}, \vec{y}) = \langle \vec{x} \cdot \vec{y} \rangle \quad (4)$$

Polynomial :

$$K(\vec{x}, \vec{y}) = \langle \vec{x} \cdot \vec{y} \rangle^d \quad (5)$$

RBF :

$$K(\vec{x}, \vec{y}) = \exp(-\gamma \|\vec{x} - \vec{y}\|), \gamma > 0 \quad (6)$$

Sigmoid :

$$K(\vec{x}, \vec{y}) = \tanh(\kappa \langle \vec{x} \cdot \vec{y} \rangle + \vartheta) \quad (7)$$

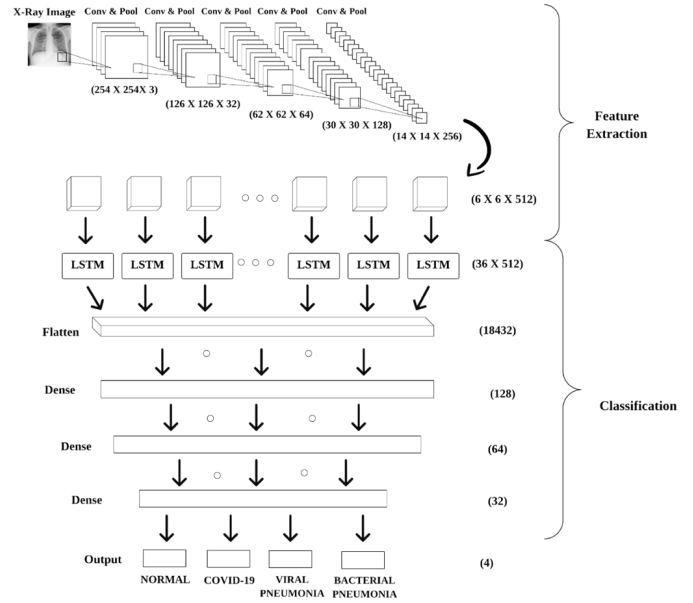


Fig. 1. Illustration of The VGG of LSTM network used for the classification of Pneumonia in this study

2) *Long-Short Term Memory(LSTM)*: The Long Short-Term Memory enhances Recurrent Neural Networks (RNNs). LSTM was created by Hochreiter & Schmidhuber (1997) and later developed and popularized by many researchers. The LSTM network can overcome the RNNs, which are problems found in the conventional, namely the vanishing gradient problem [33]. An LSTM network can remember and link previous information with currently acquired data [34]. LSTM layer consists of several units commonly called the cell. Each cell has several parts, including forget, input, and output. Where x_t represents data input; C_t and C_{t-1} sequentially symbolizes the new cell state and cell state; the previous while s_t and s_{t-1} respectively represent the current and previous output.

$$i_t = \sigma(W_i \cdot [s_{t-1}, x_t] + b_i) \quad (8)$$

$$\tilde{C}_t = \tanh(W_c \cdot [s_{t-1}, x_t] + b_c) \quad (9)$$

$$C_t = f_t x C_{t-1} + i_t x \tilde{C}_t \quad (10)$$

In the input section, certain information will be sorted and specified, updated to the section cell state using the sigmoid activation function using equation (8). A new candidate vector will be formed using the activation function tanh, added to the section cell state using the equation (9). After that, using equation (10), a new value is obtained from the input gate. This value is used to update the old cell state. In the phase, forget gate information that is less needed or has little meaning for the processed case will be removed with a sigmoid function using equation (11). In equation (12), the sigmoid activation function will produce an output value in the hidden state and put the cell state at tanh. After generating the sigmoid output and tanh output values, the two activation results are multiplied before going to the next step in equation (13).

$$f_t = \sigma(W_f \cdot [s_{t-1}, x_t] + b_f) \quad (11)$$

TABLE II
SUMMARY OF VGG-LSTM NETWORK

Layer	Type	Kernel Size	Filter	Input Shape
1.	Conv2D	2 x 2	3	255 x 255 x 3
2.	Max Pooling2D	2 x 2	-	254 x 254 x 3
3.	Conv2D	2 x 2	32	127 x 127 x 3
4.	Max Pooling2D	2 x 2	-	126 x 126 x 32
5.	Conv2D	2 x 2	64	63 x 63 x 32
6.	Max Pooling2D	2 x 2	-	62 x 62 x 64
7.	Conv2D	2 x 2	128	31 x 31 x 64
8.	Max Pooling2D	2 x 2	-	30 x 30 x 128
9.	Conv2D	2 x 2	256	15 x 15 x 128
10.	Max Pooling2D	2 x 2	-	14 x 14 x 256
11.	Conv2D	2 x 2	512	7 x 7 x 256
12.	LSTM	-	512	36 x 512
13.	FC	-	128	18432
14.	FC	-	64	128
15.	FC	-	32	64
16.	Output	-	4	32

$$o_t = \sigma(W_o \cdot [s_{t-1}, x_t] + b_o) \quad (12)$$

$$h_t = o_c \cdot \tanh(c_t) \quad (13)$$

3) *Combined VGG-LSTM*: The proposed method combines Long Short-Term Memory (LSTM) network with a pre-trained technique to detect Pneumonia based on chest X-ray images where the LSTM network is used as a classifier. The VGG techniques extract important features or information from chest X-ray images. Fig. 1 illustrates the tissue used in this study to detect Pneumonia on a chest X-ray image. The network has 16 layers: six convolutional layers, five pooling layers, 1 LSTM layer, three fully connected (dense) layers, and one output layer with the activation function softmax. Each convolution block consists of 2D convolutions and one pooling layer. A convolution layer with kernel size 2x2 is used to extract features with the ReLU activation function. While the pooling layer with a kernel size of 2x2 is used to reduce the dimensions of the input image. After passing the convolution block, the output shape will be (n,6,6,512).

On the reshape layer, the original input data is transformed into a 3D shape(36,512), and a dropout layer follows the layer LSTM with a dropout rate of 20%. After that, the chest X-ray image was classified into four categories (Normal, COVID-19 Pneumonia, Viral Pneumonia, and Bacterial Pneumonia). A summary of the network architecture used can be seen in Table 2.

III. RESULTS

This study builds a Pneumonia classification system using the algorithm Support Vector Machine, Long Short-Term Memory, and VGG-Long Short-Term Memory. Previously, to evaluate the system's performance, four performance metrics were used, including accuracy, sensitivity, specificity, and F1 score using equation (8)-(11). On the reshape layer, the original input data is transformed into a 3D shape(36,512), and a dropout layer follows the layer LSTM with a dropout

rate of 20%. After that, the chest X-ray image was classified into four categories (Normal, COVID-19 Pneumonia, Viral Pneumonia, and Bacterial Pneumonia). A summary of the network architecture used can be seen in Table 2.

$$\text{Accuracy} = \frac{(TP + TN)}{(TP + FN) + (FP + TN)} \quad (14)$$

$$\text{Sensitivity} = \frac{TP}{TP + FN} \quad (15)$$

$$\text{Specificity} = \frac{TN}{TN + FP} \quad (16)$$

$$\text{F1 Score} = \frac{2 \times TP}{(2 \times TP) + FN + FP} \quad (17)$$

$$\delta t = t_2 - t_1 \quad (18)$$

In addition to the evaluation metrics, the system performance was also compared regarding the time it takes to classify the input data represented in equation (12). The t_1 is the start time for the system to classify, and t_2 is the end time when the system has been classified. Fig. 2 shows the evaluation of the classifier's performance graphically cross-entropy (loss) in the training and testing phases. Fig. 2 (a) graphically illustrates the loss for training and validation, respectively 0.2834 and 0.4861 for LSTM architecture. Furthermore, Fig. 2 (b) graphically illustrates the loss for training and testing, respectively 0.1663 and 0.4829 for the architecture Gamma correction-LSTM.

Fig. 2 (c) graphically illustrates the loss for training and testing is 1.9104×10^{-5} and 0.4785 for VGG LSTM architecture. Furthermore, Fig. 2 (d) graphically illustrates loss for the training and testing, respectively $1,2425 \times 10^{-5}$ and 0.2117 for architecture Gamma correction-VGG-LSTM. Based on Fig. 2, we can say that the best network is the Gamma correction-VGG-LSTM network. In the 40th epoch, the Gamma correction-VGG-LSTM network has the best accuracy compared to other networks, it is proof by the accuracy network for training data is 100%, and the loss is 2.4548×10^{-5} .

Based on Tables 3 and 4, it is found that the proposed system has a fairly high accuracy, which is above 90%. And by comparing table 3 and table 4, it can be seen that the gamma correction image enhancement technique has a significant effect both in terms of accuracy, testing time, sensitivity, specificity, and F1 score. The model using gamma correction technique have higher accuracy results than model without gamma correction. Therefore, by using the gamma correction technique we can streamline the testing time. In previous studies using the same dataset obtained slightly lower accuracy with an accuracy range of 80.66%-91.62%.

In this study, we use SVM to compare the proposed method, and we also did several experiments with combination algorithms. The experimental results and details of accuracy, specificity, sensitivity, F1-Score, and time testing for each case in each network are summarized in Table 3. The SVM network achieved a specificity of 89.14%, a sensitivity of 83.12%, and an F1 score of 86.03% for COVID-19 cases. Meanwhile, the network Gamma correction SVM reached a

TABLE III
SUMMARY OF NETWORK PERFORMANCE FOR THE COVID-19 DETECTION SYSTEM WITH 3 CLASSES

Methods	Class Label	Specificity (%)	sensitivity (%)	F1-Score (%)	Accuracy (%)	Time Testing (s)
SVM	Viral Pneumonia	99.27	94.96	93.95	94.06	0.543
	COVID-19	96.05	90.55	88.89		
	Normal	93.03	95.14	95.88		
Gamma + SVM	Viral Pneumonia	99.13	96.3	93.86	94.2	0.496
	COVID-19	96.14	90.57	89.05		
	Normal	93.60	95.15	96.04		
LSTM	Viral Pneumonia	99.06	90	90.32	91.36	0.179
	COVID-19	94.12	86.81	83.36		
	Normal	89.7	92.95	94.12		
Gamma + LSTM	Viral Pneumonia	98.7	91.67	89.3	91.5	0.2
	COVID-19	94.74	86.35	84.35		
	Normal	89.55	93.12	94.16		
Deep Transfer Learning - LSTM	Viral Pneumonia	99.21	96.24	94.12	96.9	0.286
	COVID-19	97.88	97.33	95.07		
	Normal	97.66	96.85	97.87		
Gamma-Deep Transfer Learning-LSTM	Viral Pneumonia	99.56	94.32	95	97.36	0.298
	COVID-19	98.13	98.21	95.94		
	Normal	97.49	97.5	98.16		

TABLE IV
SUMMARY OF NETWORK PERFORMANCE FOR THE PNEUMONIA CLASSIFICATION SYSTEM WITH 4 CLASSES

Methods	Class Label	Specificity (%)	Sensitivity (%)	F1-Score (%)	Accuracy (%)	Time Testing (s)
SVM	Bacterial Pneumonia	77.88	86.7	82.05	88.82	0.543
	COVID-19	89.14	83.12	86.03		
	Normal	94.61	95.94	95.27		
	Viral Pneumonia	66.67	55.1	60.34		
Gamma + SVM	Bacterial Pneumonia	84.02	90.64	87.2	91.21	0.496
	COVID-19	92.45	82.7	87.31		
	Normal	94.43	97.34	95.86		
	Viral Pneumonia	78.82	68.37	73.22		
LSTM	Bacterial Pneumonia	76.78	79.8	78.26	82.59	1.307
	COVID-19	72	75.95	73.92		
	Normal	90.48	90.48	90.48		
	Viral Pneumonia	59.74	46.94	52.57		
Gamma + LSTM	Bacterial Pneumonia	77.23	76.85	77.04	83.87	0.634
	COVID-19	76.15	83.54	79.68		
	Normal	92.35	91.32	91.83		
	Viral Pneumonia	52.38	44.9	48.35		
VGG - LSTM	Bacterial Pneumonia	98.99	97.04	98.01	94.25	0.220
	COVID-19	89.7	88.19	88.94		
	Normal	94.74	95.94	95.34		
	Viral Pneumonia	91.75	90.82	91.28		
Gamma-VGG-LSTM	Bacterial Pneumonia	100	100	100	96.88	0.150
	COVID-19	92.12	93.67	92.89		
	Normal	97.75	97.34	97.54		
	Viral Pneumonia	95.88	94.9	95.38		

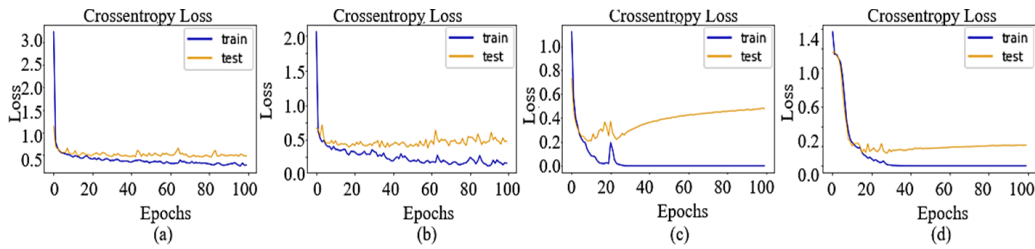


Fig. 2. Crossentropy Loss graph on the COVID-19 classification system using the network (a) LSTM (b) Gamma+LSTM (c) VGG+LSTM (d) Gamma+VGG+LSTM

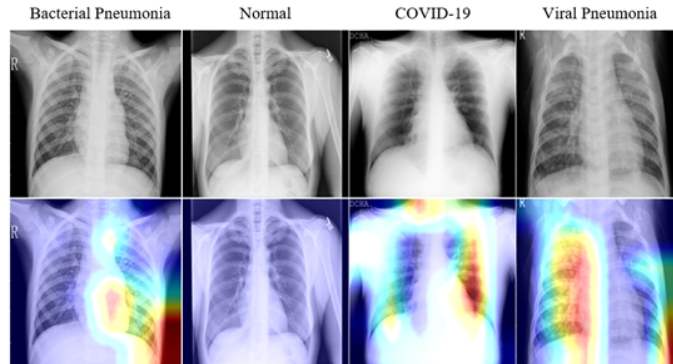


Fig. 3. Heatmap visualization on Chest X-Rays: the first row is an input image, the second row is abnormality heatmap on Chest X-Rays

TABLE V
COMPARISON OF THE COVID-19 DETECTION SYSTEM PROPOSED IN THIS STUDY WITH PREVIOUS SIMILAR STUDIES

Researcher	Dataset	Data	Network used	Accuracy
Apostolopoulos et al. [33]	Chest X-ray	3 classes (COVID-19, Normal, and Pneumonia)	VGG 19, Mobile Net V2, Inception, Xception, Inception Resnet V2	90.5 %
Li et al. [32]	Chest X-ray	3 classes (COVID-19, Normal, and Pneumonia)	DenseNet	88.9 %
proposed system	Chest X-ray	3 classes (COVID-19, Normal, Viral Pneumonia)	Gamma Correction + Deep Transfer Learning-LSTM	97.36 %
proposed system	Chest X-ray	4 classes (COVID-19, Normal, Viral Pneumonia and Bacterial Pneumonia)	Gamma Correction + Deep Transfer Learning-LSTM	96.88 %

specificity of 92.45%, a sensitivity of 82.7%, and an F1 score of 87.31% for COVID-19 cases. For the LSTM network, a specificity of 72%, a sensitivity of 75.95%, and an F1 score of 72.92% for COVID-19 issues. Meanwhile, the network Gamma correction-LSTM achieved a specificity of 76.15%, a sensitivity of 83.54%, and an F1 score of 79.68% for COVID-19 cases. The VGG-LSTM achieved a specificity of 89.7%, a sensitivity of 88.19%, and an F1 score of 88.94% for COVID-19 cases. Meanwhile, Gamma correction VGG-LSTM achieved a specificity of 92.12%, a sensitivity of 93.67%, and an F1 score of 92.89% for COVID-19 cases. Based on Table 3, The VGG-LSTM, Gamma Correction+SVM, SVM, Gamma Correction+LSTM, and LSTM networks achieve the classification accuracy of 94.25%, 91.21%, 88.82%, 83.87%, and 82.59%, respectively.

IV. DISCUSSIONS

The experimental results from Table 3 show that the evaluation results from using a combination of Gamma correction and VGG always get better results than other methods. This good result is quite reasonable because Gamma Correction can better enhance the CXR image so that the information in the image will be easier to process and the pattern contained will be easier to observe. In addition, using pre-trained techniques from VGG to extract features from CXR imagery is also very useful for capturing valuable information in each image so that the machine can better recognize each class. In this study, Gamma Correction and VGG are powerful in detecting up to four classes, including COVID-19, Bacterial Pneumonia, Viral Pneumonia, and Normal. This result is also proven in Fig. 2 shows that the training data and the data testing accuracy are not too far, so there is no overfitting. The Pneumonia classification system network with the highest accuracy in this

study is Gamma Correction+VGG-LSTM, with an accuracy of 96.88%.

Based on table 5, research conducted by Apostolopoulos et al. and Li et al. by classifying chest X-ray images into 3 classes obtained accuracy results of 90.5% and 88.9%, respectively. The same thing was done to this research, namely by using the Gamma Correction + Deep Transfer Learning-LSTM network to get higher accuracy results, namely 97.36% in experiments with 3 classes and 96.88% in experiments with 4 classes. The Deep Transfer Learning-LSTM architecture proposed in this study provides good and superior performance compared to the previous system.

In this study, the heatmap visualization on two networks with the best accuracy was performed using the Gradient-weighted Class Activation Mapping (Grad-CAM), as shown in Fig. 3. The heatmap visualization can determine how well the model classifies chest x-ray images by visualizing the affected thorax area (abnormalities). The thorax X-ray image also uses a jet color scheme in imagining the heatmap. The blue tone indicates no abnormality in the area, and the red tone suggests that the area is abnormal. This heatmap can also help us to explore abnormality and severity in some areas.

V. CONCLUSIONS

In this study, the chest X-Rays image was detected for Pneumonia diagnosis using machine learning and deep learning approaches. Based on the experimental results, it is found that the Gamma Correction+VGG-LSTM network has the highest accuracy, which is 96.88%. The accuracy value of the VGG-LSTM combined with Gamma Correction is heightened than without combined with Gamma Correction. In addition, from the experimental results that have been carried out, it can be concluded that the pre-processing stage in this study, namely gamma correction, has a significant effect on Pneumonia classification.

The comparison analysis between SVM, LSTM, and VGG LSTM on detecting the COVID-19 from chest X-ray shows that the proposed methods offer the best performances. From the experiments that have been carried out, the VGG-LSTM network has the best performance. Previously, the LSTM network had given good results in classification. Then by combining the LSTM network with a model that has been trained once for optimizing the extraction process of essential features/information in the chest X-ray image, a Pneumonia classification system with the best performance is produced, that is, Gamma Correction+VGG-LSTM. The effect of Gamma Correction in improving the image using the projection relationship between the pixel value and the gamma value is perfect.

REFERENCES

- [1] T. S. Valley, M. W. Sjoding, A. M. Ryan, T. J. Iwashyna, and C. R. Cooke, "Association of intensive care unit admission with mortality among older patients with pneumonia," *Jama*, vol. 314, no. 12, pp. 1272–1279, 2015.
- [2] R. S. Gereige and P. M. Laufer, "Pneumonia," *Pediatrics in Review*, vol. 10, no. 1, pp. 438–456, 2013.
- [3] K. Ri, "Profil kesehatan indonesia tahun 2020," *Kemendes RI*, 2021.
- [4] I. Vadász, F. Husain-Syed, P. Dorfmueller, F. C. Roller, K. Tello, M. Hecker, R. E. Morty, S. Gattenlohner, H.-D. Walrath, and F. Griminger, "Severe organising pneumonia following covid-19," *Thorax*, vol. 76, no. 2, pp. 201–204, 2021.
- [5] L. Gattinoni, S. Gattarello, I. Steinberg, M. Busana, P. Palermo, S. Lazari, F. Romitti, M. Quintel, K. Meissner, and J. J. Marini, "Covid-19 pneumonia: pathophysiology and management," *European Respiratory Review*, vol. 30, no. 162, 2021.
- [6] A. H. Attaway, R. G. Scheraga, A. Bhimraj, M. Biehl, and U. Hatipoğlu, "Severe covid-19 pneumonia: pathogenesis and clinical management," *bmj*, vol. 372, 2021.
- [7] K.-H. Yu, A. L. Beam, and I. S. Kohane, "Artificial intelligence in healthcare," *Nature biomedical engineering*, vol. 2, no. 10, pp. 719–731, 2018.
- [8] A. Zargari Khuzani, M. Heidari, and S. A. Shariati, "Covid-classifier: An automated machine learning model to assist in the diagnosis of covid-19 infection in chest x-ray images," *Scientific Reports*, vol. 11, no. 1, p. 9887, 2021.
- [9] H. Panwar, P. Gupta, M. K. Siddiqui, R. Morales-Menendez, P. Bhardwaj, and V. Singh, "A deep learning and grad-cam based color visualization approach for fast detection of covid-19 cases using chest x-ray and ct-scan images," *Chaos, Solitons & Fractals*, vol. 140, p. 110190, 2020.
- [10] Y. Oh, S. Park, and J. C. Ye, "Deep learning covid-19 features on cxr using limited training data sets," *IEEE transactions on medical imaging*, vol. 39, no. 8, pp. 2688–2700, 2020.
- [11] M. Z. Islam, M. M. Islam, and A. Asraf, "A combined deep cnn-lstm network for the detection of novel coronavirus (covid-19) using x-ray images," *Informatics in medicine unlocked*, vol. 20, p. 100412, 2020.
- [12] A. K. Das, S. Ghosh, S. Thunder, R. Dutta, S. Agarwal, and A. Chakrabarti, "Automatic covid-19 detection from x-ray images using ensemble learning with convolutional neural network," *Pattern Analysis and Applications*, vol. 24, pp. 1111–1124, 2021.
- [13] M. K. Aditi and E. Poovammal, "Image classification using a hybrid lstm-cnn deep neural network," *Int. J. Eng. Adv. Technol.*, vol. 8, no. 6, pp. 1342–1348, 2019.
- [14] S. H. Khan, A. Sohail, A. Khan, M. Hassan, Y. S. Lee, J. Alam, A. Basit, and S. Zubair, "Covid-19 detection in chest x-ray images using deep boosted hybrid learning," *Computers in Biology and Medicine*, vol. 137, p. 104816, 2021.
- [15] R. Kaur, M. Chawla, N. K. Khiva, and M. D. Ansari, "On contrast enhancement techniques for medical images with edge detection: a comparative analysis," *Journal of Telecommunication, Electronic and Computer Engineering (JTEC)*, vol. 9, no. 3-6, pp. 35–40, 2017.
- [16] T. Rahman, A. Khandakar, Y. Qiblawey, A. Tahir, S. Kiranyaz, S. B. A. Kashem, M. T. Islam, S. Al Maadeed, S. M. Zughair, and M. S. Khan, "Exploring the effect of image enhancement techniques on covid-19 detection using chest x-ray images," *Computers in biology and medicine*, vol. 132, p. 104319, 2021.
- [17] S.-C. Huang, F.-C. Cheng, and Y.-S. Chiu, "Efficient contrast enhancement using adaptive gamma correction with weighting distribution," *IEEE transactions on image processing*, vol. 22, no. 3, pp. 1032–1041, 2012.
- [18] S. Karakanis and G. Leontidis, "Lightweight deep learning models for detecting covid-19 from chest x-ray images," *Computers in biology and medicine*, vol. 130, p. 104181, 2021.
- [19] A. M. Ismael and A. Şengür, "Deep learning approaches for covid-19 detection based on chest x-ray images," *Expert Systems with Applications*, vol. 164, p. 114054, 2021.
- [20] S. Dilshad, N. Singh, M. Atif, A. Hanif, N. Yaqub, W. Farooq, H. Ahmad, Y.-m. Chu, and M. T. Masood, "Automated image classification of chest x-rays of covid-19 using deep transfer learning," *Results in physics*, vol. 28, p. 104529, 2021.
- [21] P. Pagliano, C. Sellitto, V. Conti, T. Ascione, and S. Esposito, "Characteristics of viral pneumonia in the covid-19 era: an update," *Infection*, vol. 49, pp. 607–616, 2021.
- [22] A. Giannakis, D. Mór, S. Erdmann, L. Kintzelé, R. M. Fischer, M. N. Vogel, D. L. Mangold, O. von Stackelberg, P. Schnitzler, and S. Zimmermann, "Covid-19 pneumonia and its lookalikes: How radiologists perform in differentiating atypical pneumonias," *European Journal of Radiology*, vol. 144, p. 110002, 2021.
- [23] S. Minaee, R. Kafieh, M. Sonka, S. Yazdani, and G. J. Soufi, "Deep-covid: Predicting covid-19 from chest x-ray images using deep transfer learning," *Medical image analysis*, vol. 65, p. 101794, 2020.
- [24] E. E.-D. Hemdan, M. A. Shouman, and M. E. Karar, "Covidx-net: A framework of deep learning classifiers to diagnose covid-19 in x-ray images," *arXiv preprint arXiv:2003.11055*, 2020.

- [25] X. Li, C. Li, and D. Zhu, "Covid-mobilexpert: On-device covid-19 patient triage and follow-up using chest x-rays," in *2020 IEEE international conference on bioinformatics and biomedicine (BIBM)*. IEEE, 2020, pp. 1063–1067.
- [26] I. D. Apostolopoulos and T. A. Mpesiana, "Covid-19: automatic detection from x-ray images utilizing transfer learning with convolutional neural networks," *Physical and engineering sciences in medicine*, vol. 43, pp. 635–640, 2020.
- [27] M. Loey, F. Smarandache, and N. E. M. Khalifa, "Within the lack of chest covid-19 x-ray dataset: a novel detection model based on gan and deep transfer learning," *Symmetry*, vol. 12, no. 4, p. 651, 2020.
- [28] C. Sitaula and M. B. Hossain, "Attention-based vgg-16 model for covid-19 chest x-ray image classification," *Applied Intelligence*, vol. 51, pp. 2850–2863, 2021.
- [29] G. S. George, P. R. Mishra, P. Sinha, and M. R. Prusty, "Covid-19 detection on chest x-ray images using homomorphic transformation and vgg inspired deep convolutional neural network," *Biocybernetics and Biomedical Engineering*, vol. 43, no. 1, pp. 1–16, 2023.
- [30] G. Caseneuve, I. Valova, N. LeBlanc, and M. Thibodeau, "Chest x-ray image preprocessing for disease classification," *Procedia Computer Science*, vol. 192, pp. 658–665, 2021.
- [31] S. Perumal and T. Velmurugan, "Preprocessing by contrast enhancement techniques for medical images," *International Journal of Pure and Applied Mathematics*, vol. 118, no. 18, pp. 3681–3688, 2018.
- [32] G. Mountrakis, J. Im, and C. Ogole, "Support vector machines in remote sensing: A review," *ISPRS journal of photogrammetry and remote sensing*, vol. 66, no. 3, pp. 247–259, 2011.
- [33] S. Hochreiter, "The vanishing gradient problem during learning recurrent neural nets and problem solutions," *International Journal of Uncertainty, Fuzziness and Knowledge-Based Systems*, vol. 6, no. 02, pp. 107–116, 1998.
- [34] G. Chen, "A gentle tutorial of recurrent neural network with error backpropagation," *arXiv preprint arXiv:1610.02583*, 2016.